



## Dealing with Inversion Uncertainties and Sensitivities

*John V. Pendrel, Henk J. Schouten*

CGG

### Summary

Deterministic inversion outcomes can be influenced by noise and uncertainties in the input data and also by sub-optimal inversion parameter settings. We will discuss these issues and show how they affect determinations of facies and estimations of net pay. We will also discuss the conditions under which corrections can be meaningfully made and show that some particular errors can be corrected automatically.

### Introduction

Deterministic inversions produce a single answer or in the case of AVO, a single set of elastic properties at each sample in time (or depth) and space. However, it is widely recognized that there must be some uncertainty about those values. The causes are numerous and include, noise, multiples, alignment and incident angle to name but a few. The inputs to inversion – wavelets, incident angles, low frequency models, etc. can also contribute to uncertainty. Even more worrisome, bias can be introduced. In addition to arising through the inversion inputs, bias can naturally arise as we challenge the algorithms to resolve thinner and thinner beds. The typical result is that thin layers look larger than they really are and their estimated properties are compromised. Any derivative properties created from biased inversions such as porosity will also be affected.

Apart from issues with the input data, modern inversions can involve a significant number of parameter settings in order to achieve optimum results. It can be a worrying question as to whether the User has dedicated enough diligence in the setting of the parameter values to guarantee reliable elastic properties from the inversion outcomes.

### Method

We explore the uncertainties and sensitivities described above using two QC tools. First, we retrieve the results of inversion at well locations and construct a cross-plot of inversion values vs filtered logs. The best-fit line to these data should have a slope of unity and an intercept of zero if there is no bias. The results of this analysis from each inversion test case are posted on a plot of intercept vs slope. The correlation coefficient from the best-fit analysis is represented on the plot as a bubble.

Second, we proceed with a facies analysis and subsequent probabilistic net pay calculation. We use a Bayesian approach as described by Pendrel et al., 2006. Bayes' rule maps prior probabilities to posterior probabilities, given some new evidence. The evidence is usually the results of seismic inversions or their derivatives (Pendrel et al., 2014). Log or rock physics data are cross-plotted in the inversion elastic space and elastic probability density functions (ePDFs) are designed to represent each facies under

consideration. But first we note that the scatter about the best-fit line represents cumulative uncertainty in the inversion result. The residuals from the best-fit crossplot are plotted as a histogram and modelled with their own probability density functions (uPDFs). These can be incorporated into the Bayesian analysis (Pendrel et al., 2016). Should there be bias manifested by a non-zero intercept, the mean of the uPDF will not be zero. But in these cases, that information is automatically encoded into the inputs, the data points on the elastic cross-plot are automatically relocated and the facies are therefore corrected. Now, for each inversion data sample, the ePDFs for each facies are sampled. The results are volumes of the probabilities of occurrences of each of the facies at all points in 3D space. From the facies, probabilistic net pay is calculated. The pay facies is selected and a cut-off probability assigned, below which, the particular samples in question will not be counted.

## Example

We test the above ideas with a Gulf of Mexico data set. The key horizon is the top of the Green sand which is shown in Figure 1. Below the Green horizon, we recognize both upper and lower Green sandstones. Sharp discontinuities are the results of faulting. Geologically, there is a set of two vertically-stacked deltaic systems of middle Pliocene age. They average about 400 ft. in thickness and are separated by about 500 ft. Within the play area are delta slope deformation, slump-induced turbidites, thin mouth-bed deposits but without the presence of any delta plain facies. The principle facies are Shale, Gassy Silt, Wet Sand and oily Pay sand.

The available seismic consisted of five partial-angle stacks with the maximum angle in the farthest stack being 50 degrees. A single set of wavelets, one for each partial stack, was obtained by matching elastic synthetics to the seismic at each of the seven available wells. The log sets included full-wave sonic logs over the reservoir interval, facilitating the determination of the AVO wavelets. A simultaneous AVO inversion algorithm (Pendrel et al., 2000) was used to complete the inversions. Low frequency models were structurally-compliant, facies-based constant trends interactively defined at horizons.

The results of the relative (no low frequencies) simultaneous inversion with optimum parameter settings are shown in Figure 2 along an arbitrary line passing through all the wells. Band-pass-filtered logs are overlaid. The matches are not perfect since the inversion has no prior knowledge of the high frequency component of the logs. The region of interest is the Green sand (between the orange arrows). The P Impedance agreement with the wells is good and the  $V_p/V_s$  fair.

Using the Bayesian procedure, facies were determined throughout the seismic volume. The inputs were P Impedance and  $V_p/V_s$  from the simultaneous AVO inversion. The log facies have been overlaid for comparison at the well locations. The agreement is generally good, especially for the prospective facies. Probabilistic net pay maps were created for the upper sand. The cut-off used was 0.90.

Figure 3 shows the intercept-slope results for relative P Impedance and  $V_p/V_s$  for a wide range of cases. The figure tests inversion inputs wavelet phase and scale, NMO and angle of incidence. Parameters tested are seismic S/N, reflection sparsity, rock property constraints and expected deviations from the input low frequency trends. The largest effects on P Impedance come from wavelet phase and scale and incident angle. The correlations are not much affected, indicating that corrections could be possible. In the  $V_p/V_s$  cross-plot, NMO and incident angle were important. NMO errors also resulted in very low correlations, making any kind of correction recovery impossible. Note that for these 4ms data, significant correlation reduction occurred at errors of only 4ms and dramatically so at 8ms. The clear message is that alignment is important. These effects also manifested on the net pay maps, as expected. Figure 4

compares net pay from the optimum inversion to the case of a -4ms alignment error on the far stack. The net pay is dramatically reduced. The above tests were also done for the absolute inversions (not shown).

### Conclusions

We have demonstrated that cross plotting relative inversion properties at well locations vs band-passed-filtered logs is a viable QC for a wide range of potential problems. The derivative effects of data and parameter uncertainties can be dramatic but sometimes reversible. In facies estimation, certain types of bias problems are automatically corrected when uncertainty-bias analysis has been done and employed.

### Acknowledgements

The authors wish to thank Stone Energy for permission to show these data. They also thank their colleagues in the CGG GeoSoftware team for their valuable comments and support.

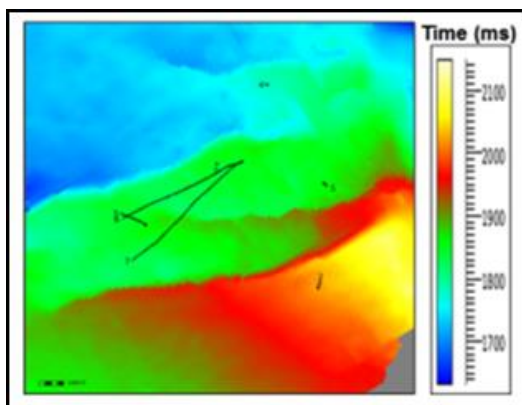


Figure 1: Project map showing the green horizon and the well locations

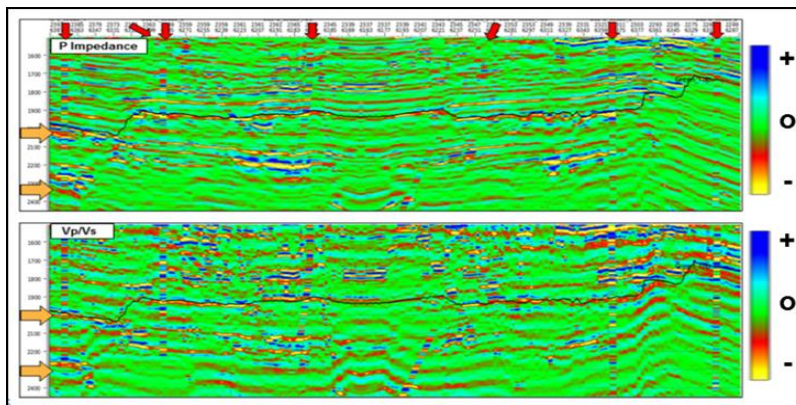


Figure 2: P Impedance and Vp/Vs from a relative inversion. Band-pass-filtered logs are overlain at the well locations (red arrows). The inversion algorithm was blind to the wells..

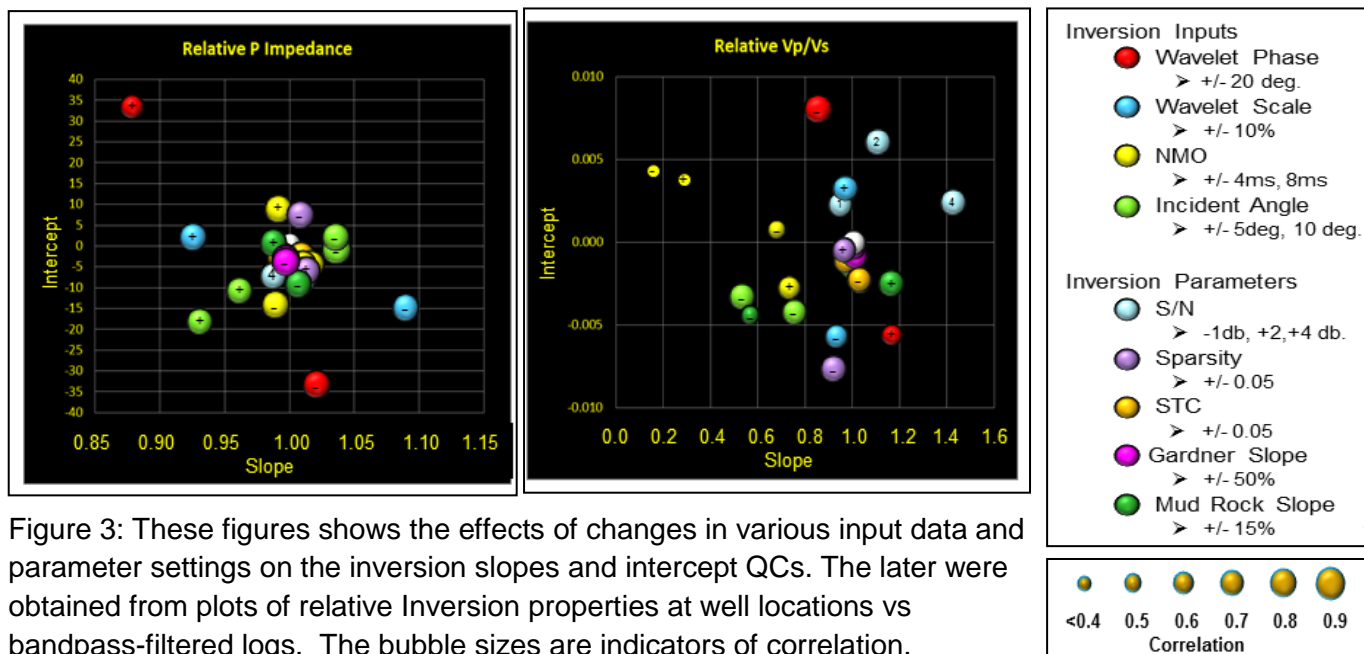


Figure 3: These figures shows the effects of changes in various input data and parameter settings on the inversion slopes and intercept QCs. The later were obtained from plots of relative Inversion properties at well locations vs bandpass-filtered logs. The bubble sizes are indicators of correlation.

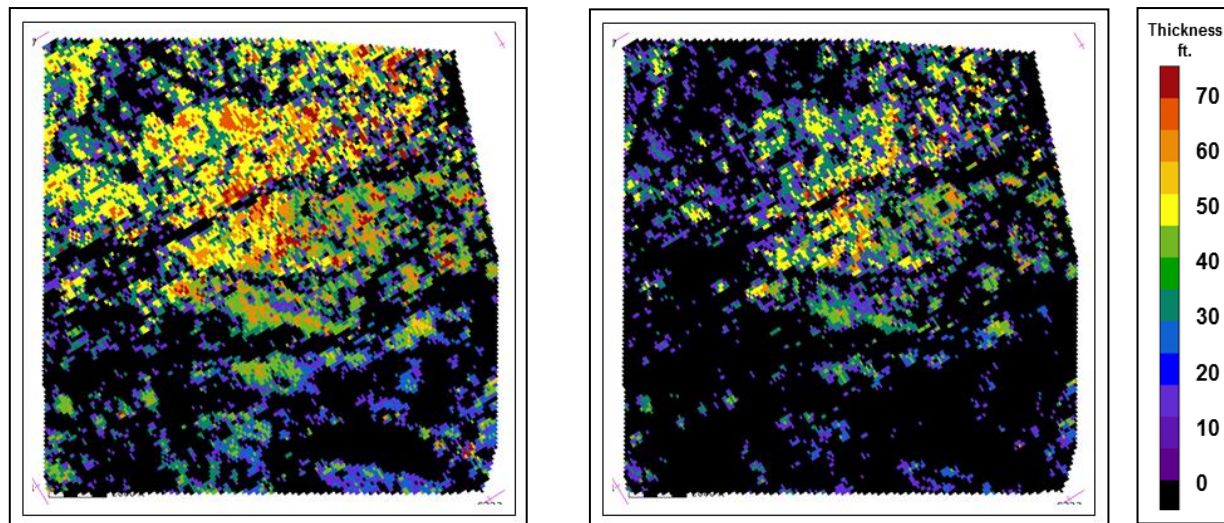


Figure 4: This figure compares net pay from the optimum inversion (left) with that from an inversion wherein the far partial stack was misaligned by -4ms (right). The Net Pay is dramatically reduced.

#### References

- Pendrel, J., Debeye, H., Pedersen-Tatalovic, R., Goodway, B., Dufour, J., Bogaards, M., Stewart, R., 2000, Estimation and interpretation of P and S Impedance volumes from the simultaneous inversion of P-wave offset data, CSEG Ann. Mtg. Abs.
- Pendrel, J., Mangat, C., Feroci, M., 2006, Using Bayesian inference to compute facies-fluids probabilities, CSEG Ann. Mtg. Abs
- Pendrel, J., Marini, A.I., 2014, Static models for unconventional reservoirs: a Barnett shale case study, SEG Summer Workshop Abs., San Diego
- Pendrel, J., Schouten, H.J., Bornard, R., (2016), Accounting for bias and uncertainty in facies estimations from deterministic inversions, SEG Ann. Mtg. Abs., p 2876-2880